NANO LETTERS

Letter

pubs.acs.org/NanoLett

Coherent Optical Transitions in Implanted Nitrogen Vacancy Centers

Y. Chu,*[,†,#] N.P. de Leon,[†,#,∥] B.J. Shields, B. Hausmann,[‡] R. Evans,[†] E. Togan,[¶] M. J. Burek,[‡] M. Markham,[§] A. Stacey,[§] A.S. Zibrov,[†] A. Yacoby,[†] D.J. Twitchen,[§] M. Loncar,[‡] H. Park,[†,∥] P. Maletinsky,[⊥] and M.D. Lukin[†]

[†]Department of Physics, Harvard University, Cambridge, Massachusetts 02138, United States

[‡]School of Engineering and Applied Science, Harvard University, Cambridge, Massachusetts 02138, United States

[¶]Institute for Quantum Electronics, ETH-Zurich, CH-8093 Zurich, Switzerland

[§]Element Six Ltd, Kings Ride Park, Ascot, Berkshire SL5 8BP, United Kingdom

[∥]Department of Chemistry and Chemical Biology, Harvard University, Cambridge, Massachusetts 02138, United States

[⊥]Department of Physics, University of Basel, 4056 Basel, Switzerland

ABSTRACT: We report the observation of stable optical transitions in nitrogen-vacancy (NV) centers created by ion implantation. Using a combination of high temperature annealing and subsequent surface treatment, we reproducibly create NV centers with zero-phonon lines (ZPL) exhibiting spectral diffusion that is close to the lifetime-limited optical line width. The residual spectral diffusion is further reduced by using resonant optical pumping to maintain the NV^- charge state. This approach allows for placement of NV centers with excellent optical coherence in a well-defined device layer, which is a crucial step in the development of diamond-based devices for quantum optics, nanophotonics, and quantum information science.

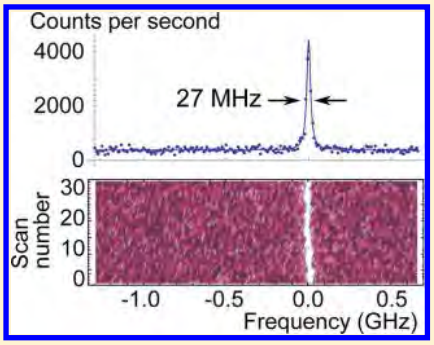

KEYWORDS: *nitrogen vacancy center, spectral diffusion, diamond, implantation, annealing, surface treatment*

The negatively charged nitrogen vacancy (NV) center in diamond is a solid-state system that combines excellent spin coherence with atomic-like optical transitions at cryogenic temperatures. Because of these properties, the NV center has emerged as a promising candidate for the realization of unique applications in the fields of quantum information, quantum optics, and metrology.[1−3] Although many of these applications make use of coherent interactions between light and NV centers,[4−6] the optical transitions of atom-like solid-state systems are generally imperfect because of the influence of the solid state environment. In particular, the energies of the NV center's optically excited states are highly sensitive to local electric fields. Therefore, fluctuations in the charge environment around the NV center cause fluctuations in the frequency of the optical transition. This phenomenon, which is referred to as spectral diffusion, is a generic effect associated with optical transitions in atom-like solid-state systems.[7,8] Techniques to suppress and eliminate spectral diffusion are currently being actively explored.[5,9,10]

To investigate the optical properties of NV centers, photoluminescence excitation (PLE) studies are typically performed by repeatedly scanning a resonant excitation laser through the NV center's zero-phonon line (ZPL).[9−16] A 532 nm laser is applied at the end of each scan to reverse potential photoionization of the NV center caused by the resonant laser. For a single PLE scan, one typically observes a narrow resonance. A nearly lifetime-limited single-scan line width of 16 MHz has been reported in a single diamond nanocrystal,[11] and a lifetime-limited single-scan line width of 13 MHz was measured for a native NV center inside a natural diamond sample.[12] However, these measurements of the single-scan line width exclude the effects of spectral diffusion. It was observed that the narrow resonance jumps to a different frequency for each successive PLE scan, indicative of local charge fluctuations caused by the repumping laser.[11,13,14] Previously, it has been shown that off-resonant excitation can photoionize localized defects inside and on the surface of the diamond crystal, leading to the observed spectral jumps.[9,17] When the NV center is monitored over long time scales, such behavior results in an overall line width that can be much larger than the single-scan line width. This long-term, extrinsically broadened line width, rather than the single-scan line width, is the limiting factor for most applications requiring spectral stability. For example, remote entanglement of NV centers relies on interference of photons with well-defined matching frequencies.[5] Efficient photonic devices such as single photon switches and transistors make use of strong NV−photon interactions and require that the emitters remain on resonance with the incident light.[18] Therefore, a number of different techniques have been explored to reduce the effects of spectral diffusion, including active

Received: December 31, 2013
Revised: February 15, 2014
Published: March 3, 2014

 © 2014 American Chemical Society

stabilization and preselection of the transition frequency.[5,10] However, all of these techniques increase the technical complexity and limit the repetition rate of the experiments. The "on demand" creation of emitters with inherently low spectral diffusion under repeated excitation over long time scales is an outstanding challenge in implementing scalable applications using quantum optics with atom-like systems.

Because one-of-a-kind natural diamond samples, such as the one investigated in ref 12, cannot be used as reproducible starting materials for scalable systems, recent experiments have made use of NV centers incorporated into high quality synthetic diamond during the growth process.[5,10,16] In addition to imperfections in their optical coherence, NV centers introduced during the diamond growth process are limited in their usefulness due to their low concentration and random locations. For example, in order to incorporate NV centers into nanophotonic or nanomechanical devices, it is necessary to develop a method to create a controllable concentration of emitters in a well-defined device layer while maintaining their excellent optical properties.

The key idea of this work is to create NV centers in a surface layer that exhibit coherent optical transitions with nearly lifetime-limited linewidths even under the effects of spectral diffusion. We accomplish this by first introducing NV centers at a well-defined and controllable depth using ion implantation.[19] We then demonstrate how to suppress the fundamental cause of spectral diffusion by creating a diamond environment that is nearly free of defects that contribute to charge fluctuations. This is achieved through a combination of annealing and surface treatments. Finally, we further improve the optical properties of the NV centers by combining our approach with a recently developed technique for preventing photoionization of the remaining charge traps.[14]

Figure 1 summarizes the experimental procedure to create shallow implanted NV centers with narrow optical lines. As our

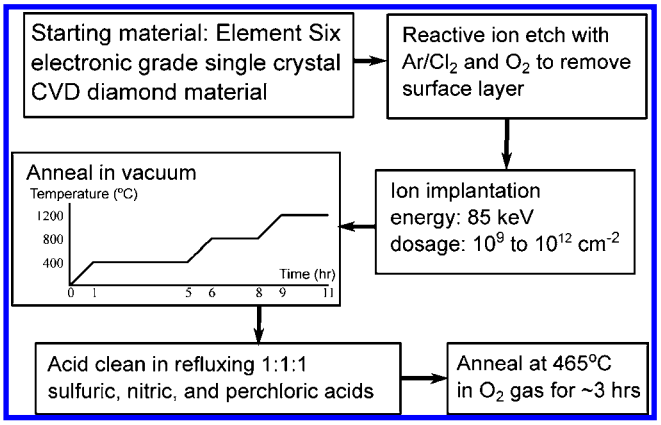

Figure 1. Procedure for creating spectrally stable NV centers through ion implantation, annealing, and surface treatment. The Ar/Cl_2 (O_2) etch was done using an ICP power of 400 W (700 W), a RF power of 250 W (100 W), a DC bias of 423 V (170 V), a chamber pressure of 8 mTorr (10 mTorr), and a gas flow rate of 25/40 sccm (30 sccm). The sample temperature was set to 17 °C.

starting material, we use single crystal diamond from Element Six grown using microwave-assisted chemical vapor deposition (CVD). The single crystal samples were homoepitaxially grown on specially prepared ⟨100⟩ oriented synthetic diamond substrates, taking care to ensure that the surface quality of the substrates was as high as possible to reduce sources of dislocations. The CVD synthesis was performed using conditions as described in refs 20 and 21. The resultant diamond material is measured using electron paramagnetic resonance (EPR) to have a nitrogen concentration of less than 5 parts per billion. The surface layer of these samples is generally damaged and highly strained because of mechanical polishing. Therefore, we first remove the top several micrometers of the sample using a 30 min Ar/Cl_2 etch followed by a 20 min O_2 etch in an UNAXIS Shuttleline inductively coupled plasma reactive ion etcher. We then implant $^{15}N^+$ ions at an energy of 85 keV at a variety of doses from $10^9/cm^2$ to $10^{12}/cm^2$. According to simulations done using the Stopping and Range of Ions in Matter (SRIM) software, this should result in a mean nitrogen stopping depth of ∼100 nm with a straggle of ∼20 nm.[22] $^{15}N^+$ were used instead of $^{14}N^+$ so that, if needed, we could distinguish NV centers formed from implanted nitrogen versus native nitrogen through electron spin resonance measurements. Subsequently, we anneal the implanted samples under high vacuum ($P \lesssim 10^{-6}$ Torr). Our standard annealing recipe consists of a 4 h at 400 °C step, a 2 h at 800 °C step, and a 2 h at 1200 °C step, with a 1 h ramp up to each temperature. It is important that a good vacuum is maintained throughout the annealing process because diamond etches and graphitizes under residual oxidizing gases at such high temperatures.[23] Following the anneal, we remove graphitic carbon and other surface contaminants by cleaning the diamonds for one hour in a 1:1:1 refluxing mixture of sulfuric, nitric, and perchloric acids. Finally, we perform a 465 °C annealing in an O_2 atmosphere in a rapid thermal processor (Modular Process Technology, RTP-600xp) in three 48 min steps following the recipe used in ref 24. This oxygen annealing is believed to remove sp^2-hybridized carbon and result in a more perfect oxygen termination of the surface than acid cleaning alone. We have observed that it enhances charge stability in the NV^- state and helps to reduce blinking and photobleaching.

We investigate the resulting NV centers using a low-temperature confocal microscopy setup, where the diamond samples are cooled to <10 K in a helium flow cryostat (Janis ST-500). Figure 2a shows confocal photoluminescence (PL) images taken with ∼1 mW 532 nm laser excitation for four different implantation doses. An implantation dose of $10^9/cm^2$ results in a very low density of NV centers, which is comparable to the native NV concentration in some electronic grade samples. A dose of $10^{12}/cm^2$ results in a high density layer of completely unresolvable NV centers. At an intermediate dose of $10^{10}/cm^2$, however, we obtain resolvable single NV centers with a density on the order of 1 NV/μm^2, implying a conversion efficiency of ∼1%. Comparing the fluorescence intensity to the single NV count rate, we can roughly estimate that, in the $10^{11}/cm^2$ sample, there are ∼10 NV centers per focal spot, whereas in the $10^{12}/cm^2$ sample, there are ∼100 NV centers per focal spot. We note that the conversion efficiency is somewhat lower than previously reported values, which could result from differences in starting material, dose calibration, and annealing procedures.[19]

In Figure 2b, we present corresponding ZPL spectra of NV centers for the three highest implantation doses. The spectra were taken by scanning an external cavity diode laser around 637.2 nm while collecting fluorescence in the phonon-sideband (PSB). Excitation at 532 nm was performed at each point of the scan to alleviate the effects of photoionization during resonant excitation. Without such repumping to maintain the charge state, we find that most NV centers remain in the NV^- charge

dx.doi.org/10.1021/nl404836p | Nano Lett. 2014, 14, 1982−1986

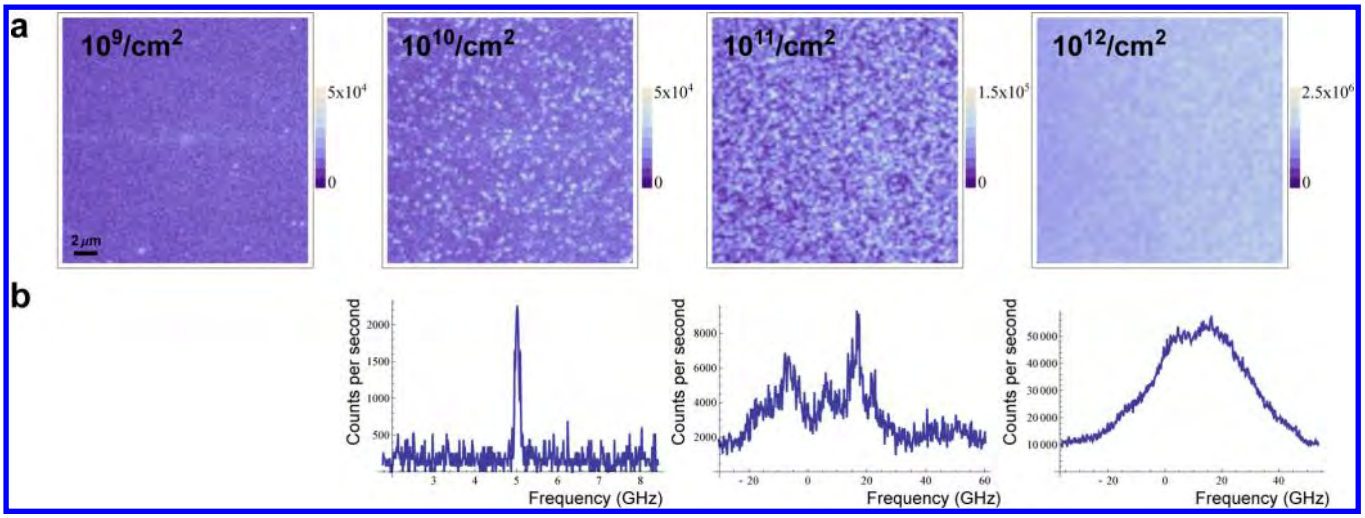

Figure 2. (a) Confocal PL images of the implanted layer of NV centers for four different nitrogen ion doses. (b) Corresponding representative PLE spectra for the three highest doses. Each spectrum is the average of ∼10 PLE scans.

state for a few PLE scans and demonstrate almost no spectral diffusion. Subsequently, the NV center ionizes and remains dark. We emphasize here that Figure 2b and Figure 3b–d

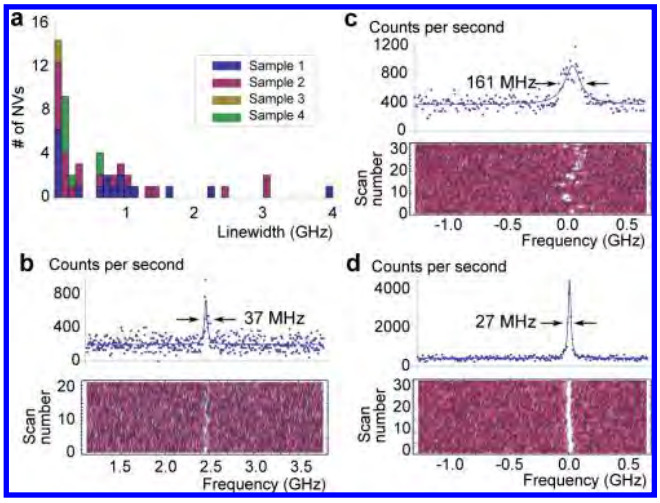

Figure 3. (a) Histogram of linewidths for NV centers in four samples implanted with a dose of $10^{10}/cm^2$ using 532 nm excitation to repump the NV into the negative charge state. (b) Spectrum showing the narrowest line width from panel a (top) obtained by averaging twenty-one successive PLE scans (bottom). Each scan takes ∼2 s. (c) Spectrum of another NV taken using 532 nm repump (top). Corresponding single PLE scans illustrating spectral jumps due to repumping (bottom). (d) Spectrum of the same NV as in panel c taken using 575 nm resonant excitation of the NV^0 state to repump back into NV^-.

present spectra that are averages of many successive laser scans taken over the course of minutes. Therefore, they are indicative of the spectral stability of NV centers over both short and long time scales and include all effects of spectral diffusion caused by the repumping laser. Beyond these time scales, longer-term drifts of the NV frequency can be easily compensated by electric fields or tuning the excitation frequency with minimal cost to the experimental repetition rate. At a dose of $10^{10}/cm^2$, most single NV centers exhibit narrow PLE lines. As the dose increases to $10^{11}/cm^2$, the spectra show multiple features with several broader peaks. Finally, at $10^{12}/cm^2$, the spectrum is a mostly featureless peak several tens of gigahertz wide. We note here that the spectra for the two highest doses exhibit the effects of both increased single NV center linewidths and the presence of several NV centers in the focal spot. If the linewidths were comparable to the $10^{10}/cm^2$ sample, we should be able to observe a collection of narrow resonances spread over the scan range. However, this is not the case, which is an indication that increased nitrogen concentration in the environment of the NV center leads to additional spectral diffusion. Indeed, the substitutional nitrogen defect has an ionization energy threshold of 2.2 eV and, therefore, can be photoionized with 532 nm light, which has an energy of 2.33 eV/photon.[25]

From this point on, we focus on samples implanted with a dose of $10^{10}/cm^2$. Figure 3a shows a histogram of linewidths for 50 NV centers in four such samples. Although there is a range of linewidths, a majority of NV centers exhibit linewidths less than 500 MHz, which is comparable to naturally occurring NV centers deep inside electronic grade CVD diamond.[5] This is an indication that we have eliminated most impurities with fluctuating charge states in the vicinity of the NV centers, which may include both impurities on the nearby surface and defects inside the diamond introduced by the implantation process. In Figure 3b, we present an example spectrum of the narrowest line width we have observed, along with the results of 21 successive PLE scans to demonstrate the long-term stability of the transition line. Our measured line width of 37 ± 5 MHz under conventional 532 nm repumping is, to the best of our knowledge, a record for the extrinsically broadened line width of NV centers.

To further reduce residual spectral diffusion of the NV centers, we incorporate a technique recently demonstrated in ref 14. Instead of using 532 nm light to repump the NV^0 state into NV^-, we use a home-built tunable frequency doubled external cavity diode laser operating at 575 nm to resonantly excite the NV^0 ZPL, which has been shown to efficiently convert the NV center back to the negatively charged state even at very low powers. The 575 nm laser was turned on and scanned across the NV^0 ZPL between each frequency scan of the 637 nm spectroscopy laser. As was also demonstrated in ref 14, this method results in a drastic reduction of the spectral diffusion because of the lower incident intensity and energy per

dx.doi.org/10.1021/nl404836p | Nano Lett. 2014, 14, 1982–1986

photon of the 575 nm excitation (2.16 eV/photon) compared to the conventional 532 nm excitation. For example, the NV center shown in Figure 3c has a NV^- ZPL line width of 161 MHz using 532 nm excitation. The line width was reduced to 27 MHz using the 575 nm repumping technique (Figure 3d).

We now discuss our sample preparation process in more detail and propose a mechanism for the creation of optically stable NV centers through high temperature annealing. In general, annealing is required after ion implantation to mobilize vacancies such that they combine with the nitrogen atoms to form NV centers. In addition, the annealing process causes other defects to become mobile at particular temperatures and potentially migrate to the surface, effectively repairing any damage to the crystal caused by implantation. Earlier works have employed a range of different annealing temperatures, typically in the range between 400 and 1000 °C. Several temperature steps in this range were shown to enable specific mechanisms important to the efficient formation of stable NV centers. In particular, at 400 °C, earlier work has indicated that vacancies and interstitial nitrogen atoms introduced by implantation migrate and annihilate with each other.[26] At 800 °C, vacancies become mobile and combine with nitrogen atoms on lattice sites to form NV centers, which then remain stable.[27] At temperatures much less than 800 °C, this process is too slow to allow NV formation in a reasonable time period. At temperatures much higher than 800 °C, the vacancies are highly mobile, but there is an indication that the rate of NV formation is suppressed.[28] This could be because of the higher thermal energy in the diamond lattice, which causes the local strain field around the isolated nitrogen defects to becomes less efficient at trapping migrating vacancies.

At even higher temperatures, additional defects such as divacancies, sp^2 type defects, and hydrogen become mobile and anneal out.[27,29,30] Recent work has demonstrated that annealing at a temperature of 1200 °C significantly improved the coherence properties of implanted NV centers.[31] This indicates that some of the remaining defects after 800 °C annealing are paramagnetic. The electronic and optical properties of these defects, such as the level structure and ionization energies, have generally not been well studied. However, we have briefly investigated the optical properties of samples annealed without the 1200 °C step and found that, although a few NV centers had linewidths greater than several hundred megahertz, most had PLE lines that were too broad to be discernible. These results provide evidence that annealing at high temperatures eliminates localized defects that can affect the optical properties of NV centers. The exact structure and properties of these defect states remain to be determined through, for example, EPR measurements, optical spectroscopy, and ab initio calculations of energy level structures.

Our work shows that it is possible to create implanted NV centers with excellent optical coherence properties, opening up a large range of possibilities for future studies and applications. In addition to a better understanding of the material and defect properties that contribute to spectral diffusion, there are many other aspects and parameters of our technique that remain to be explored. For example, as mentioned above, we believe that high temperature annealing is crucial for the creation of high quality NV centers. However, it may be possible to modify the exact temperature and time of each annealing step to achieve similar or even better results. Furthermore, though we have not extensively studied the dependence of optical coherence on implantation depth, there is evidence that reasonably stable transitions are possible with much shallower NV centers. We have observed linewidths of a few hundred megahertz from several NV centers in a diamond sample created by implantation with a nitrogen dose of $10^{11}/cm^2$ at an energy of 6 keV, giving a nominal depth of 10 nm. This also indicates that our sample processing method does not remove more than a few nanometers from the diamond surface. Further systematic studies on the effect of implantation energy, dose, and annealing recipes are needed to explore the possibility of creating optically coherent NV centers in high densities or very close to the diamond surface for applications such as coupling of multiple NV centers and electric field sensing.

Another important application that has recently become the focus of much effort is the implementation of nanoscale photonic structures to tailor the interaction of light and NV centers.[32] Thus far, all previous demonstrations of diamond-based photonic structures have used diamond materials with a high density of native NV centers whose linewidths are generally many gigahertz or more.[32,33] To realize quantum nanophotonic devices in a deterministic, scalable fashion, it is important to begin with a bulk material that contains very high quality emitters in a well-defined device layer. For this reason, the ability to controllably create NV centers with inherently good optical coherence, which we have demonstrated in this work, is a crucial step for the practical development of many diamond-based quantum nanophotonic devices and scalable quantum technologies.

AUTHOR INFORMATION

Corresponding Author

*Y. Chu. E-mail: ychu@physics.harvard.edu.

Author Contributions

#Y.C. and N.P.d.L. contributed equally to this work.

Notes

The authors declare no competing financial interest.

ACKNOWLEDGMENTS

We thank F. Jelezko for many fruitful discussions and for sharing the ideas on NV^0 repumping technique with us. Etching and postprocessing of diamond samples were performed in the Center for Nanoscale Systems at Harvard. This work was supported by the NSF, CUA, the DARPA QuASAR and SPARQC programs, and the STC Center for Integrated Quantum Materials, NSF Grant No. DMR-1231319. Y.C. and R.E. acknowledge financial support from the NSF GRFP. N.P.d.L. acknowledges financial support from the Element Six postdoctoral fellowship. B.H. and Y.C. acknowledge financial support from HQOC.

REFERENCES

(1) Bernien, H.; Hensen, B.; Pfaff, W.; Koolstra, G.; Blok, M. S.; Robledo, L.; Taminiau, T. H.; Markham, M.; Twitchen, D. J.; Childress, L.; Hanson, R. *Nature* **2013**, *497*, 86−90.

(2) Balasubramanian, G.; Chan, I. Y.; Kolesov, R.; Al-Hmoud, M.; Tisler, J.; Shin, C.; Kim, C.; Wjcik, A.; Hemmer, P. R.; Krueger, A.; Hanke, T.; Leitenstorfer, A.; Bratschitsch, R.; Jelezko, F.; Wrachtrup, J. *Nature* **2008**, *455*, 648−651.

(3) Maurer, P. C.; Kucsko, G.; Latta, C.; Jiang, L.; Yao, N. Y.; Bennett, S. D.; Pastawski, F.; Hunger, D.; Chisholm, N.; Markham, M.; Twitchen, D. J.; Cirac, J. I.; Lukin, M. D. *Science* **2012**, *336*, 1283−1286.

(4) Togan, E.; Chu, Y.; Trifonov, A. S.; Jiang, L.; Maze, J.; Childress, L.; Dutt, M. V. G.; Sorensen, A. S.; Hemmer, P. R.; Zibrov, A. S.; Lukin, M. D. *Nature* **2010**, *466*, 730−734.
(5) Bernien, H.; Childress, L.; Robledo, L.; Markham, M.; Twitchen, D.; Hanson, R. *Phys. Rev. Lett.* **2012**, *108*, 043604.
(6) Sipahigil, A.; Goldman, M. L.; Togan, E.; Chu, Y.; Markham, M.; Twitchen, D. J.; Zibrov, A. S.; Kubanek, A.; Lukin, M. D. *Phys. Rev. Lett.* **2012**, *108*, 143601.
(7) Robinson, H. D.; Goldberg, B. B. *Phys. Rev. B* **2000**, *61*, R5086−R5089.
(8) Ambrose, W. P.; Moerner, W. E. *Nature* **1991**, *349*, 225−227.
(9) Bassett, L. C.; Heremans, F. J.; Yale, C. G.; Buckley, B. B.; Awschalom, D. D. *Phys. Rev. Lett.* **2011**, *107*, 266403.
(10) Acosta, V. M.; Santori, C.; Faraon, A.; Huang, Z.; Fu, K.-M. C.; Stacey, A.; Simpson, D. A.; Ganesan, K.; Tomljenovic-Hanic, S.; Greentree, A. D.; Prawer, S.; Beausoleil, R. G. *Phys. Rev. Lett.* **2012**, *108*, 206401.
(11) Shen, Y.; Sweeney, T. M.; Wang, H. *Phys. Rev. B* **2008**, *77*, 033201.
(12) Tamarat, P.; Gaebel, T.; Rabeau, J. R.; Khan, M.; Greentree, A. D.; Wilson, H.; Hollenberg, L. C. L.; Prawer, S.; Hemmer, P.; Jelezko, F.; Wrachtrup, J. *Phys. Rev. Lett.* **2006**, *97*, 083002.
(13) Fu, K.-M. C.; Santori, C.; Barclay, P. E.; Rogers, L. J.; Manson, N. B.; Beausoleil, R. G. *Phys. Rev. Lett.* **2009**, *103*, 256404.
(14) Siyushev, P.; Pinto, H.; Vörös, M.; Gali, A.; Jelezko, F.; Wrachtrup, J. *Phys. Rev. Lett.* **2013**, *110*, 167402.
(15) Orwa, J. O.; Santori, C.; Fu, K. M. C.; Gibson, B.; Simpson, D.; Aharonovich, I.; Stacey, A.; Cimmino, A.; Balog, P.; Markham, M.; Twitchen, D.; Greentree, A. D.; Beausoleil, R. G.; Prawer, S. *J. Appl. Phys.* **2011**, *109*, 083530.
(16) Stacey, A.; Simpson, D. A.; Karle, T. J.; Gibson, B. C.; Acosta, V. M.; Huang, Z.; Fu, K. M. C.; Santori, C.; Beausoleil, R. G.; McGuinness, L. P.; Ganesan, K.; Tomljenovic-Hanic, S.; Greentree, A. D.; Prawer, S. *Adv. Mater.* **2012**, *24*, 3333−3338.
(17) Aslam, N.; Waldherr, G.; Neumann, P.; Jelezko, F.; Wrachtrup, J. *New J. Phys.* **2013**, *15*, 013064.
(18) Chang, D. E.; Sorensen, A. S.; Demler, E. A.; Lukin, M. D. *Nat. Phys.* **2007**, *3*, 807−812.
(19) Pezzagna, S.; Naydenov, B.; Jelezko, F.; Wrachtrup, J.; Meijer, J. *New J. Phys.* **2010**, *12*, 065017.
(20) Isberg, J.; Hammersberg, J.; Johansson, E.; Wikstršm, T.; Twitchen, D. J.; Whitehead, A. J.; Coe, S. E.; Scarsbrook, G. A. *Science* **2002**, *297*, 1670−1672.
(21) Markham, M.; Dodson, J.; Scarsbrook, G.; Twitchen, D.; Balasubramanian, G.; Jelezko, F.; Wrachtrup, J. *Diamond Relat. Mater.* **2011**, *20*, 134−139.
(22) Ziegler, J. F. Particle Interactions With Matter. http://www.srim.org (accessed June 20, 2013).
(23) Seal, M. *Phys. Status Solidi B* **1963**, *3*, 658−664.
(24) Fu, K.-M. C.; Santori, C.; Barclay, P. E.; Beausoleil, R. G. *Appl. Phys. Lett.* **2010**, *96*, 121907.
(25) Rosa, J.; Vanecek, M.; Nesladek, M.; Stals, L. *Diamond Relat. Mater.* **1999**, *8*, 721−724.
(26) Twitchen, D.; Hunt, D.; Wade, C.; Newton, M.; Baker, J.; Anthony, T.; Banholzer, W. *Phys. B* **1999**, *273 - 274*, 644−646.
(27) Twitchen, D. J.; Newton, M. E.; Baker, J. M.; Anthony, T. R.; Banholzer, W. F. *Phys. Rev. B* **1999**, *59*, 12900−12910.
(28) Twitchen, D. J.; Markham, M. Element Six Ltd., Ascot, U.K. Personal communication, 2013.
(29) Lea-wilsonf, M. A.; Lomer, J. N.; Van Wyk, J. A. *Philos. Mag. B* **1995**, *72*, 81−89.
(30) Talbot-Ponsonby, D. F.; Newton, M. E.; Baker, J. M.; Scarsbrook, G. A.; Sussmann, R. S.; Whitehead, A. J. *Phys. Rev. B* **1998**, *57*, 2302−2309.
(31) Naydenov, B.; Reinhard, F.; Laemmle, A.; Richter, V.; Kalish, R.; D'Haenens-Johansson, U. F. S.; Newton, M.; Jelezko, F.; Wrachtrup, J. *Appl. Phys. Lett.* **2010**, *97*, 242511.
(32) Faraon, A.; Santori, C.; Huang, Z.; Acosta, V. M.; Beausoleil, R. G. *Phys. Rev. Lett.* **2012**, *109*, 033604.
(33) Babinec, T. M.; Hausmann, B. J. M.; Khan, M.; Zhang, Y.; Maze, J. R.; Hemmer, P. R.; Loncar, M. *Nat. Nanotechnol.* **2010**, *5*, 195−199.